

# The Angular Correlation Function of $K' \sim 19.5$ Galaxies and the Detection of a Cluster at $z = 0.775$

Nathan Roche<sup>1,4</sup>, Stephen A. Eales<sup>1,5</sup>, Hans Hippelein<sup>2,6</sup>  
and Chris J. Willott<sup>3,7</sup>

<sup>1</sup> Department of Physics and Astronomy, University of Wales Cardiff, P.O. Box 913, Cardiff CF2 3YB, Wales.

<sup>2</sup> Max Planck Institut für Astronomie, Königstuhl 17, 69117 Heidelberg, Germany.

<sup>3</sup> Department of Astrophysics, University of Oxford, Nuclear and Astrophysics Laboratory, Keble Road, Oxford OX1 3RH, England.

<sup>4</sup> ndr@astro.cf.ac.uk    <sup>5</sup> sae@astro.cf.ac.uk    <sup>6</sup> hippelei@mpia-hd.mpg.de    <sup>7</sup> c.willott1@physics.ox.ac.uk

18 May 2019

## ABSTRACT

On five  $K'$ -band ( $2.1\mu\text{m}$ ) Omega camera images, covering a total of  $162.2 \text{ arcmin}^2$  to a completeness limit  $K' \simeq 19.5$ , we investigate (i) the clustering environment of a sample of 5 radio galaxies at  $0.7 \leq z \leq 0.8$  and (ii) the galaxy angular correlation function,  $\omega(\theta)$ . Applying two methods – counting galaxies within 1.5 arcmin of each radio galaxy, and using a cluster detection routine with a modelled cluster profile – we detect a cluster of estimated Abell richness  $N_A = 85 \pm 25$  (class 1 or 2), approximately centred on the radio galaxy 5C6.75 at  $z = 0.775$ . Of the other radio galaxies, two appear to be in less rich groups or structures, and two in field environments. The mean clustering environment of all 5 radio galaxies is estimated to be of  $N_A = 29 \pm 14$  richness, similar to that of radio galaxies at more moderate redshifts of  $0.35 < z < 0.55$ .

The angular correlation function,  $\omega(\theta)$ , of the detected galaxies shows a positive signal of  $\sim 4\sigma$  significance at limits  $K' = 18.5\text{--}20.0$ . The relatively high amplitude of  $\omega(\theta)$  and its shallow scaling with magnitude limit are most consistent with a pure luminosity evolution model in which E/S0 galaxies are much more clustered than spirals ( $r_0 = 8.4$  compared to  $4.2 h^{-1} \text{ Mpc}$ ) and clustering is approximately stable ( $\epsilon \sim 0$ ) to  $z \sim 1\text{--}2$ .

We also find a significant excess of close (1.5–5.0 arcsec separation) pairs of galaxies compared to the expectation from the inward extrapolation of  $\omega(\theta)$ . To  $K' = 19.5$ , we estimate that  $11.2 \pm 3.4$  per cent of galaxies belong to excess close pairs. This can be explained if the local rate of galaxy mergers and interactions increases with redshift as  $\sim (1+z)^m$  with  $m = 1.36_{-0.50}^{+0.35}$ .

## Key words:

galaxies: clusters: general – galaxies: active – infrared: galaxies

## 1 INTRODUCTION

Statistical measures of the clustering of distant galaxies, and the identification of rich galaxy clusters at high redshifts, are both of great importance in the study of galaxy evolution and the formation of structure in the Universe. The clustering of galaxies on the sky, as described in terms of the angular correlation function,  $\omega(\theta)$ , has been studied extensively in galaxy surveys at  $\lambda \simeq 0.4\text{--}0.9 \mu\text{m}$  wavelengths. The amplitude of  $\omega(\theta)$  decreases on going faintward approximately as expected if galaxies undergo moderate luminosity evolution while their intrinsic clustering remains approximately stable in proper co-ordinates (e.g. Roche et al. 1996; Roche and Eales 1998; Postman et al. 1998).

It is now possible to survey sufficiently large areas at near infra-red wavelengths, e.g. the  $2.2\mu\text{m}$   $K$ -band, to measure the galaxy  $\omega(\theta)$  amplitude (Baugh et al. 1996; Carlberg et al. 1997). Near-IR surveys, compared to those at visible light wavelengths, contain a much larger proportion of early-type galaxies and are less sensitive to the effects of increased star-formation in the past, so may be useful in studying the evolution of clustering separately from that of the star-formation rate. Previously (Roche, Eales and Hippelein 1998, hereafter Paper I), we measured the  $\omega(\theta)$  amplitude at a  $K = 20$  limit on 17 small fields totalling  $101.5 \text{ arcmin}^2$ . The relatively high amplitude of  $\omega(\theta)$  compared to that on deep blue-band surveys (e.g. Roche et al. 1996) sug-

gested the intrinsic clustering of red E/S0 galaxies is strong ( $r_0 \simeq 8 h^{-1}$  Mpc) compared to that of spirals, and that clustering is approximately stable ( $\epsilon \simeq 0$ ) with redshift, but more data was needed to obtain better statistics.

Some faint galaxy surveys have shown an excess in the number of very close ( $\leq 6$  arcsec separation) pairs of galaxies compared to the number expected from  $\omega(\theta)$  at larger scales (e.g. Infante, de Mello and Menanteau 1996). The excess pairs appear to be galaxies undergoing mergers or interaction, and the number observed suggested some increase with redshift in the merger/interaction rate. Estimation of the merger rate evolution is of cosmological interest (Carlberg, Pritchett and Infante 1994), but there have been large differences between the numbers of excess close pairs seen on different datasets. In Paper I we found an excess of 2–3 arcsec separation pairs on the fields observed with the Redeye camera but not on those observed with the Magic camera, while the larger  $R \leq 23.5$  survey of Roche and Eales (1998) found a significant excess of 2–5 arcsec pairs on one  $1.01 \text{ deg}^2$  area but no excess on another  $0.75 \text{ deg}^2$  area. These inconsistencies might be explained by differences in seeing and instrumental resolution, but to confirm the earlier results it is important to investigate the close pair statistics on further deep surveys.

The detection of rich clusters of galaxies at high redshifts ( $z > 0.5$ ) is also of great interest, as their number, richness and other properties may provide important constraints on cosmological parameters (e.g. Eke, Cole and Frenk 1996). At visible light wavelengths, the contrast of clusters against the background and foreground galaxies falls steeply with increasing redshift, making detection difficult at  $z > 0.6$  – but this is in part due to the strong k-correction dimming of early-type galaxies. In the  $K$ -band, the k-correction actually produces a brightening to  $z \sim 1$ , so most high redshift cluster members will have very red  $R - K$  colours and clusters should be detectable on  $K$ -band images to significantly higher redshifts. Near-IR observations have already found rich clusters at redshifts as high as  $z = 1.27$  (Stanford et al. 1997) and possibly at  $z = 2.39$  (Waddington 1998).

Searches for high redshift clusters have often concentrated on areas containing high redshift QSOs or radio galaxies, as some of these sources do lie in rich clusters and the AGN provides an easily measured redshift. The clustering environment of radio galaxies is of interest in itself for understanding their evolution. At low redshifts the more luminous (FRII) radio galaxies are generally found in field environments, whereas at  $z \sim 0.5$ , luminous radio galaxies are found in similar numbers in the field and in rich clusters, with the average environment being approximately that of an Abell class 0 cluster (Yates, Miller and Peacock 1989; Hill and Lilly 1991).

Yee and Ellingson (1993) explained this as an environmental influence on radio galaxy evolution, causing sources in clusters to decrease much more rapidly in radio luminosity at  $z \leq 0.5$  than those in the field. Wan and Daly (1996) found no observable differences between the properties of powerful radio galaxies in field and cluster environments, and concluded that the change in radiogalaxy environment with redshift is most likely due to an evolution of the clusters themselves – an increase in the typical intra-cluster medium pressure between  $z \sim 0.5$  and  $z \sim 0$  might suppress FRII activity in most lower redshift rich clusters and allow only

the less radioluminous FRI outbursts to occur. However, to better understand this process, it is important to determine whether there is any further change in the mean radio galaxy environment at  $z > 0.5$ .

In Paper I, 17 high redshift ( $z_{mean} = 1.1$ ) 6C radio galaxies were cross-correlated with the surrounding  $K < 20$  galaxies to estimate their mean clustering environment. The mean radiogalaxy-galaxy cross-correlation function showed no significant signal, but provided upper limits which were consistent with a mean radio galaxy environment similar to that at  $z \sim 0.5$  (i.e. Abell 0 clusters) but argued against a much richer environment (i.e. Abell 2 clusters). However, at similar redshifts, some of the more radioluminous 3CR galaxies are in rich clusters. e.g. Deltorn et al. (1997) confirmed that 3CR184 at  $z = 0.996$  was in rich cluster thought to be of Abell class 2, and Bowes and Smail (1997) detected a massive cluster centred on 3C336 at  $z = 0.927$  from its gravitational lensing.

In this paper we investigate the clustering environment of 5 radio galaxies at  $0.7 \leq z \leq 0.8$ , using  $K$ -band images obtained using the large format Omega camera on Calar Alto. The more moderate radiogalaxy redshifts and the much larger field areas compared to the study of Paper I should greatly improve our chances of finding clusters. Section 2 describes the observational data and the detection of galaxies and stars. We investigate the environment of the radiogalaxies before the analysis of  $\omega(\theta)$ , as the presence of very rich clusters might affect the interpretation of the  $\omega(\theta)$  (see Paper I). We describe the modelling of distant clusters in Section 3.2 and search for clusters centred on the radio galaxies using two methods, described in Sections 3.3 and 4 respectively. In Section 5 we investigate the galaxy  $\omega(\theta)$  and compare it with models and previous observations. In Section 6 we investigate the number of close pairs of galaxies. Section 7 discusses the implications of these results and the conclusions are briefly summarized in Section 8.

## 2 DATA

### 2.1 Observations

Our dataset consists of images of 5 fields, each centred on a radio galaxy at  $0.7 \leq z \leq 0.8$  (Table 1). One source is from the 6C catalog of radio galaxies with 151 MHz fluxes of at least 2.2 Jy, the other four from the 7C catalog (Willott et al. 1998, and in preparation) with a fainter flux limit of 0.5 Jy (these have names beginning ‘5C’, as they were first detected in a 5C survey). These 7C galaxies have radio luminosities  $L(151\text{MHz}) \simeq 10^{27.6} \text{ WHz}^{-1}$ , much lower than 3C galaxies but above the FRII/FRI divide. The five galaxies were selected from the catalogs solely on the basis of being in the desired redshift range, so should be an unbiased sample of  $0.7 \leq z \leq 0.8$  radio galaxies.

The fields were observed in the  $2.1\mu\text{m}$   $K'$ -band (Wainscoat and Cowie 1992) on the nights of 13 and 14 December 1997, using the Omega wide-field near-infrared camera at the prime focus of the 3.5m Calar Alto telescope (Sierra de los Filabres, Andalucia, Spain). This has a  $1024 \times 1024$  pixel HgCdTe (1–2.5  $\mu\text{m}$ ) array with pixelsize 0.3961 arcsec. Each field was exposed for 30 seconds 120 times, and the 120 exposures stacked together and flat-fielded during the observing run. For the purposes of flat-fielding, the 120 exposures

**Table 1.** Positions (equinox 2000.0), spectroscopic redshifts and  $K'$  magnitudes (as measured from this data) of the five radio galaxies

Galaxy	R.A.	Dec.	$z$	$K'$
5C6.25	02:10:24.45	+34:10:46.0	0.706	17.44
5C6.29	02:11:05.85	+32:56:44.2	0.720	16.61
5C6.43	02:12:02.69	+34:02:18.1	0.775	17.95
5C6.75	02:14:01.20	+30:26:14.3	0.775	17.05
6C0822	08:25:47.36	+34:24:26.5	0.700	17.48

were slightly offset in a grid pattern, reducing the areas of the final images (in which all pixels have a full 60 minutes exposure) to approximately  $870 \times 870$  pixels or  $5.75 \times 5.75$  arcmin.

## 2.2 Source detection

The Starlink PISA (Position, Intensity and Shape Analysis) package, developed by M. Irwin, P. Draper and N. Eaton, was used to detect and catalog the objects. The chosen detection criterion was that a source must exceed an intensity threshold of  $1.5\sigma$  above the background noise ( $\sigma$  being determined by PISA), corresponding to  $21.0 K'$  mag arcsec $^{-2}$  on these five images, in at least 5 connected pixels. As in Paper I, PISA was run with deblend (objects connected at the detection threshold may be split if they are separate at a higher threshold) and the ‘total magnitudes’ option. There were a total of 3160 detections.

Detections in four circular ‘holes’ (radius 9 to 20 arcsec) around bright, saturated stellar images were excluded in order to remove spurious noise detections, leaving a total 162.3 arcmin $^2$  area of usable data. Radial profiles were fitted to several non-saturated stars on each image using ‘pisafit’, and from these profiles the average resolution on the reduced images was estimated as  $FWHM = 1.13 \pm 0.06$  arcsec. Star-galaxy separation was performed using plots of central against total intensity, normalized to the ratio from the fitted stellar profile. On these plots the stellar locus was separable from the galaxies to  $K' \sim 17$ , and a total of 185 detections to this limit were classed as stars. All fainter objects were assumed to be galaxies, but we later apply corrections to our results for the effects of faint star contamination.

## 2.3 Galaxy and star counts

Figure 1 shows the differential number counts, in  $\Delta(K') = 0.5$  mag bins, of objects classed as galaxies on these images, with field-to-field error bars. These are compared with galaxy counts from Paper I and a number of other  $K$ -band surveys, plotted here assuming a mean colour  $K' = K + 0.13$ . The plot also shows the predictions of a non-evolving and a pure luminosity evolution (PLE) model. The models assume  $q_0 = 0.05$  and are the same as those of Roche and Eales (1998) but computed in the  $K'$ -band rather than the  $R$ -band.

To  $K' \simeq 19.5$ , our galaxy counts agree well with those from Paper I and from previous surveys, including those using much deeper data, suggesting that our galaxy detection is virtually complete to this limit. Our counts level out at  $19.5 < K' < 20.0$  and fall off at  $K' > 20$ . On the basis of the

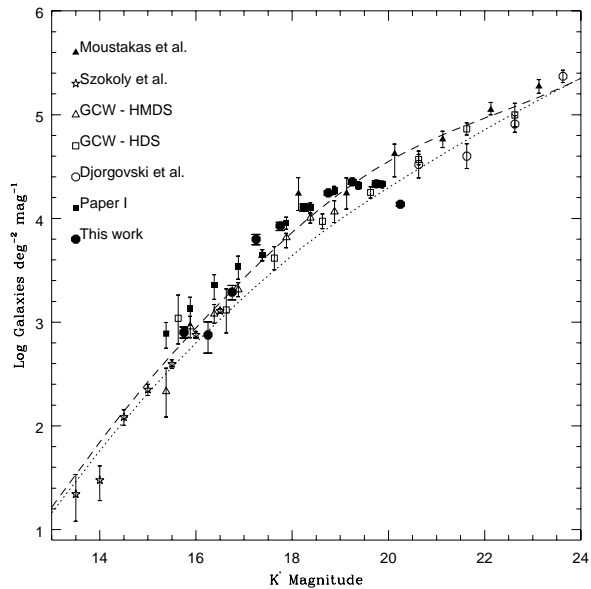


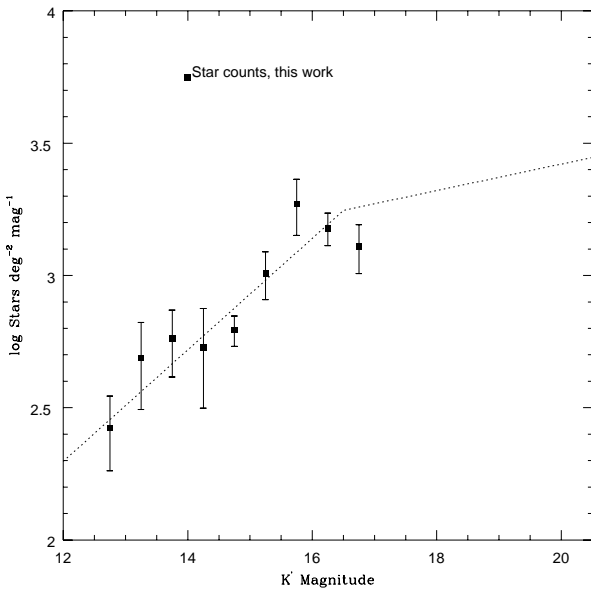
**Figure 1.** Differential galaxy number counts, in 0.5 mag intervals of  $K'$  magnitude, for our five fields compared to our Paper I and the  $K$ -band surveys of Gardner, Cowie and Wainscoat (1993), Djorgovski et al. (1995), Moustakas et al. (1997) and Szokoly et al. (1998), together with the predictions of  $q_0 = 0.05$  PLE (dashed) and non-evolving (dotted) models.

count gradient from models and deeper data ( $\gamma \simeq 0.30$ ), our galaxy detection is  $\sim 32\%$  incomplete at  $19.5 < K' < 20$ . Figure 1 also shows the  $K$  and  $K'$ -band number counts to be generally in good agreement with this PLE model over the entire  $\sim 10$  mag range.

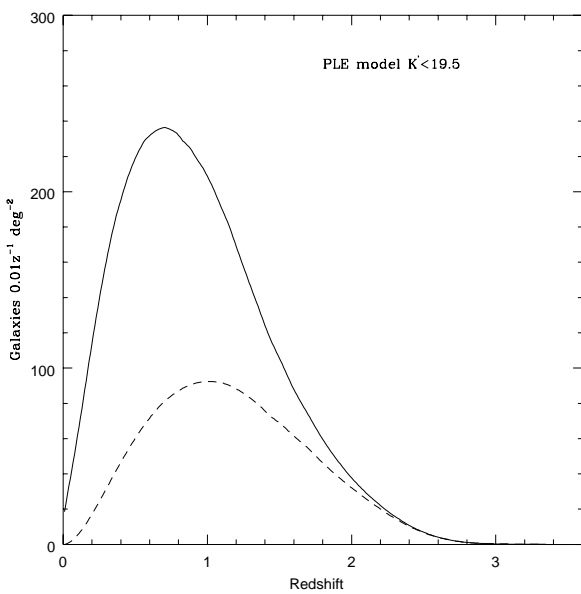
Figure 2 shows the number counts of objects classed as stars, with field-to-field errors. The star count at  $13 < K' < 16.5$  was best-fitted with  $\log N_{stars} = -0.231 + 0.2107K'$ , but at fainter magnitudes the star count will flatten to a slope closer to  $\gamma = 0.05$ , as in the model used by Couch, Jercevic and Boyle (1993). Following Roche and Eales (1998), we derive a conservative estimate of faint-star contamination by (i) assuming stars are classified correctly to  $K' = 16.5$  (ii) extrapolating the fitted power-law with  $\gamma = 0.05$  at  $K' > 16.5$  (as shown on the plot), (iii) summing the extrapolated star counts from  $K' = 16.5$  to the magnitude limit being considered, but subtracting the number of  $16.5 < K' < 17$  detections (29) already classified as stars. In this way, we estimate that about 256 of the 1626 detections classed as  $K' \leq 19.5$  galaxies are actually stars.

Figure 3 shows the PLE model prediction for the redshift distribution  $N(z)$  at the  $K' = 19.5$  limit. The predicted mean redshift is 0.94, the radio galaxy redshifts are close to the peak of  $N(z)$ , and we expect to see galaxies to  $z \sim 2.5$ , with E/S0 galaxies predominating at  $z > 1$ .

## 3 CLUSTERING AROUND THE RADIO GALAXIES



**Figure 2.** Differential star number counts in 0.5 mag intervals of  $K'$  magnitude, with the power-law fitted at  $13 < K' < 16.5$  (dashed line) and the extrapolation with a  $\gamma = 0.05$  slope at  $K' > 16.5$ .



**Figure 3.** Redshift distribution predicted by our PLE model for all galaxies (solid) and E/S0 galaxies only (dashed) to  $K' = 19.5$ .

### 3.1 Visual impression

Before any detailed modelling of galaxy clusters, we examine our data by eye to see whether there are obvious associations around any of the radio galaxies. Figure 4 shows maps of the distribution of  $K' \leq 19.5$  galaxies on each of the five fields, with the radiogalaxies indicated. The images provide more information than these maps as connecting filaments

and interactions between galaxies may be visible. The visual impression is that

(i) The radio galaxy 5C6.25 appears to lie on a long *S*-shaped filament, but as a large proportion of these galaxies are in filaments, this may not necessarily indicate an especially clustered environment.

(ii) The radio galaxy 5C6.29 is not obviously in any sort of association (the four bright galaxies nearby are almost certainly at much lower redshift).

(iii) 5C6.43 has a close companion of similar brightness ( $K' = 18.01$ ), 6.4 arcsec away, with some signs of an interaction, but it is not obviously part of any larger group.

(iv) 5C6.75 lies within a more compact *S*-shaped structure, some 1 arcmin across with at least 10 bright members and a number of faint galaxies in the same area. The region around the radio galaxy contains many interacting pairs and small groups of galaxies. The concentration of galaxies is obvious on Figure 3 and seems a good candidate for being a true cluster.

(v) 6C0822 has two close companions of similar brightness and may be part of an interacting group of several galaxies, although this association appears less rich than that around 5C6.75.

Hence the radio galaxies appear to be in a wide range of environments, with evidence of clustering in some cases. To quantify this, we consider a model of a rich cluster placed at the radio galaxy redshifts.

### 3.2 Cluster modelling

One measure of the richness of a galaxy cluster is the ‘Abell richness’  $N_A$  defined as the number of cluster members with apparent magnitudes no more than 2.0 magnitudes fainter than the third-ranked cluster member (e.g. Abell et al. 1989). Rich clusters are defined as those with  $N_A \geq 30$ , with  $30 \leq N_A \leq 49$  being Abell class 0,  $50 \leq N_A \leq 79$  class 1 and  $80 \leq N_A \leq 129$  class 2.

Hereafter,  $h$  is Hubble’s constant in units of  $100 \text{ km s}^{-1} \text{Mpc}^{-1}$ . The surface density of galaxies in rich clusters, in terms of the projected distance from the centre  $r = \theta d_A$ , typically follows a profile of the form

$$\rho(r) = \frac{\rho_0}{[1 + (r/R_c)^2]^\alpha} \quad (1)$$

out to  $r_{max}$  where  $\rho(r)$  falls to zero. Following Kepner et al. (1998) we assume a core radius  $R_c = 0.1 h^{-1} \text{ Mpc}$  and  $\alpha = 0.75$ , which are approximately in the middle of the ranges observed for both local and distant clusters (Girardi et al. 1995; Lubin and Postman 1996). With  $q_0 = 0.05$ , a proper distance  $1.0h^{-1} \text{ Mpc}$  at  $0.7 \leq z \leq 0.8$  corresponds to 3.38–3.57 arcmin, so an Omega image should contain almost the entirety of any cluster centred on a radio galaxy.

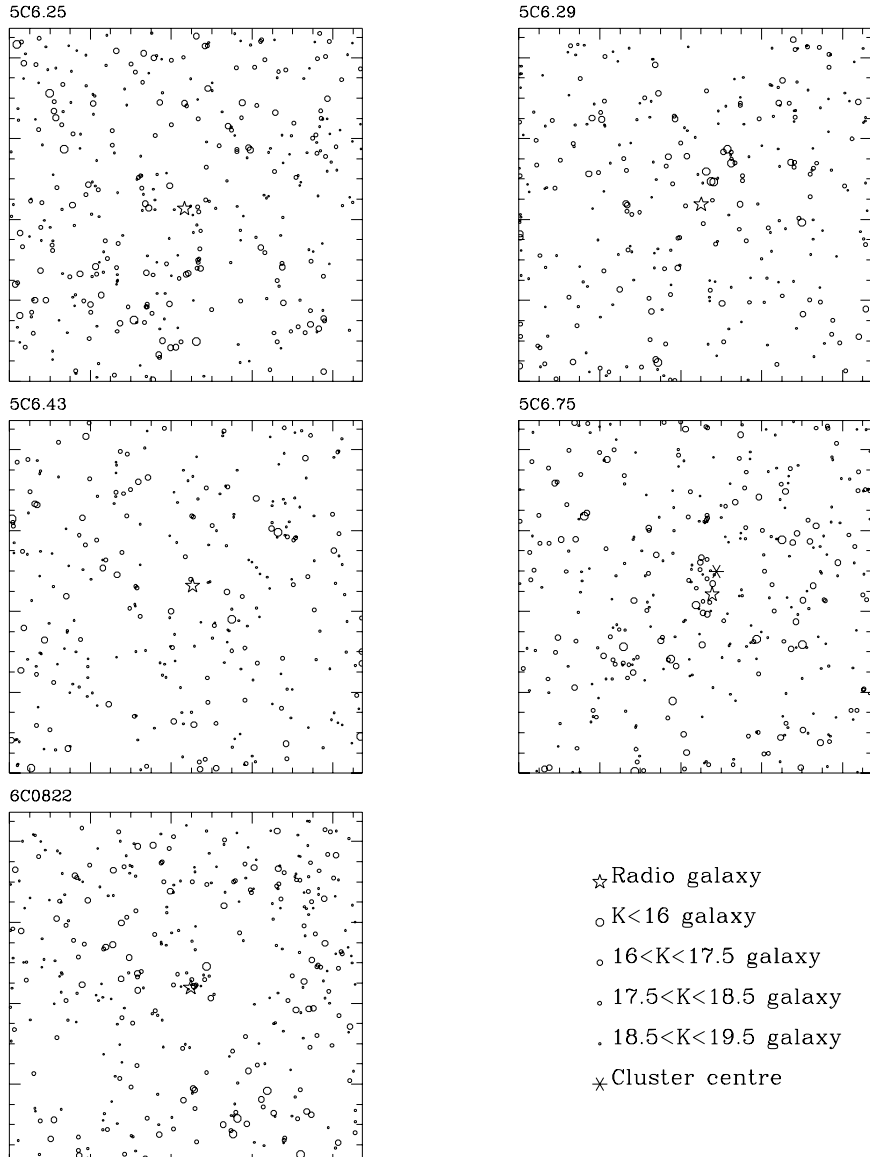


**Figure 4.** Positions of all  $K' \leq 19.5$  galaxies on the five Omega fields, each  $5.75 \times 5.75$  arcmin. The best-fit cluster centre on 5C6.75 is shown by an asterisk.

For field galaxies, we assumed a luminosity function, derived from the Las Campanas redshift survey, with a much steeper faint-end slope for blue than for red galaxies. However, rich clusters contain a much higher proportion of early-type galaxies than the field population, with large numbers of low luminosity red galaxies. For example, Oemler et al. (1997) estimated that only 12 per cent of the galaxies in two high density Abell class 1 clusters at  $z \sim 0.4$  were much bluer than passively evolving ellipticals. To take this into account, when modelling the cluster we assumed the k+e-corrections and colours of an evolving S0 model for a large proportion (78 per cent) of the galaxies in the luminosity functions corresponding to Sab and later types, to give a total red galaxy fraction  $\sim 88$  per cent.

Kepner et al. (1998) parameterized the richness of model clusters in terms of their total luminosity within  $r_{max}$ , and estimated that this luminosity (hereafter  $L_{cl}$ , in units of  $L^*$ ) related to the Abell richness as  $N_A \simeq \frac{2}{3}L_{cl}$ . We determine  $L_{cl}$  for our model clusters by summing the luminosity of the cluster galaxies (to a faint limit  $K' = 22$ ) relative to  $L^*$  (hence  $L_{cl}$  is not affected by luminosity evolution).

When modelled clusters are placed at the redshifts of the radio galaxies, we estimated the number of cluster members that would be visible to the completeness limit of  $K' = 19.5$  as  $\sim 0.7\text{--}0.8L_{cl}$ , with about half of these lying within 1.5 arcmin of the cluster centre. At  $z \simeq 0.75$ , an  $L^*$  elliptical ( $M_{K'} = -24.85$  for  $h=0.5$ ) evolving as in our PLE model would have an apparent magnitude  $K' \simeq 18.0$  and a typical brightest cluster galaxy ( $M_{K'} = -26.49$  for  $h = 0.5$ , Collins and Mann 1998) would have  $K' \simeq 16.4$ , so it is almost certain that any galaxies associated with the radio galaxies will be fainter than  $K' = 16$ . We first estimate the cluster environment of the radio galaxies simply by counting the number of  $16 \leq K' \leq 19.5$  galaxies within 1.5 arcmin of the radiogalaxy positions and comparing with modelled clusters.

### 3.3 Excess galaxies within 1.5 arcmin

Table 2 gives the total number of  $16 \leq K' \leq 19.5$  galaxies within 1.5 arcmin of each of the radio galaxy positions (including the radio galaxies themselves),  $N(< 1.5)$ . The background galaxy density is estimated for each field from the number of galaxies  $> 1.5$  arcmin from the radio galaxy,  $N(> 1.5)$ , divided by the area of the part of the field  $> 1.5$  arcmin from the radio galaxy,  $A(> 1.5)$ . The excess above the background of galaxies up to 1.5 arcmin from the radio galaxy is first estimated by subtracting

$$N(< 1.5) - \frac{\pi(1.5)^2}{A(> 1.5)}N(> 1.5) \quad (2)$$

However, this background density may be an overestimate, as with the profile from equation (1) about half the members of any cluster will lie  $> 1.5$  arcmin from the cluster centre. For a modelled cluster of richness  $L_{cl}$ , we can estimate a corrected background density by subtracting the number of model cluster galaxies  $> 1.5$  arcmin from the cluster centre,  $C(> 1.5)$ , from the observed  $N(> 1.5)$ . This leads to a higher, corrected estimate of the excess of galaxies  $< 1.5$  arcmin from the radio galaxy,

**Table 2.** The number of  $16 \leq K' \leq 19.5$  galaxies within 1.5 arcmin of the radio galaxy positions (within 1.0 arcmin in the case of 6C0822), the excess above the background density (equation 2), the excess corrected for the presence of a cluster (equation 3), and the estimated total luminosity  $L_{cl}$  of a cluster centred on the radio galaxy. Errors are  $\sqrt{N}$ .

Galaxy	$N_{gal}$	Excess	Corrected excess	$L_{cl}$
5C6.25	82	$11.5 \pm 9.1$	$15.8 \pm 12.5$	$40 \pm 32$
5C6.29	69	$8.2 \pm 8.3$	$11.5 \pm 11.6$	$30 \pm 31$
5C6.43	62	$4.1 \pm 7.9$	$5.4 \pm 10.4$	$15 \pm 29$
5C6.75	98	$33.5 \pm 9.9$	$45.0 \pm 13.3$	$125 \pm 37$
6C0822	36	$1.6 \pm 6.0$	$2.0 \pm 7.5$	$8 \pm 28$

$$N(< 1.5) - \frac{\pi(1.5)^2}{A(> 1.5)}[N(> 1.5) - C(> 1.5)] \quad (3)$$

The cluster richness is then estimated as the value of  $L_{cl}$  for which the modelled number of cluster members within 1.5 arcmin of the cluster centre,  $C(< 1.5)$ , is equal to the corrected richness estimate for the same model cluster. For these fields, the background correction effectively increases the estimates of  $L_{cl}$  by  $\sim 35$  per cent. 6C0822 actually gave a negative excess at  $< 1.5$  arcmin, probably as a result of large-scale structure of foreground galaxies, so to reduce the effects of this we compute the excess for a smaller radius of 1.0 arcmin.

Of the 5 radio galaxies, only 5C6.75 shows a significant excess of nearby galaxies over the scales expected for a rich cluster. This excess would correspond to a cluster of Abell richness  $N_A \simeq 83 \pm 25$ , i.e. Abell class 1 or 2. On the basis of  $\sqrt{N}$  statistics the significance is  $3.4\sigma$ , although this may be an overestimate as galaxy clustering increases the variance of counts-in-cells. Whereas 5C6.25 did appear to be in some sort of large-scale association, its estimated richness is probably less than that needed for it to be described as a cluster ( $L_{cl} \simeq 45$ ), and whereas 6C0822 did appear to be in an association of a few galaxies the lack of any excess over arcmin scales indicates this to be a small isolated group rather than a true cluster. For the five radio galaxies, the mean  $L_{cl}$  is  $43.6 \pm 21.1$ , corresponding to a mean Abell richness  $29 \pm 14$ . The significance of this mean value is discussed in Section 7.1.

Of course, it is possible that clusters are not exactly centred on the radio galaxies. It would be advantageous to determine the true centres of any clusters, estimate the richness using the full model profile of equation (1) rather than just its summation to 1.5 arcmin, and verify that detection is significant after taking into account the clustering of background galaxies. All these are possible using a second method of searching for clusters, described below.

## 4 CLUSTER DETECTION

### 4.1 Method

We search the regions near the radio galaxies for clusters using a cluster detection routine which is essentially a simplified version of the Adaptive Matched Filter technique described by Kepner et al. (1998). The profile of a cluster of chosen redshift  $z$  and richness  $L_{cl}$  is modelled as in Section 3.2. For a chosen position  $(x,y)$ , the number of

$16 \leq K' \leq 19.5$  galaxies are counted in annular bins of  $\Delta(\theta) = 10$  arcsec centred on  $(x,y)$ . The number of galaxies in a model cluster, placed at  $(x,y)$ , are counted in the same annular bins, with areas missed off the edges of the field or lost due to ‘holes’ taken into account. The model and observed counts are then compared by summing

$$\chi^2(x, y, L_{cl}, z) = \frac{1}{n_b - 1} \sum_{i=1}^{i=n_b} \frac{(C_i - N_i + A_i \rho_{back})^2}{A_i \rho} \quad (4)$$

where  $C_i$  is the number of galaxies in bin  $i$  in the modelled cluster,  $N_i$  is the observed number of galaxies in bin  $i$ ,  $A_i$  is the area of bin  $i$  (taking into account any area lost due to holes or the field edges),  $\rho$  the mean surface density of galaxies on the whole field and  $\rho_{back}$  a corrected background density (the observed number of galaxies on the field minus the total number that would be in the modelled cluster, divided by the field area).

The  $\chi^2$  statistic is computed for a grid of  $(x,y)$  positions on each field, for a model cluster with  $z$  equal to the radio galaxy redshift and  $L_{cl} = 125$ , representing the divide between Abell classes 1 and 2 and the approximate richness of the 5C6.75 cluster. For each field  $\rho(\chi^2)$  is computed as the scatter in  $\chi^2$  values between 4900  $(x,y)$  positions, thus taking into account both the non-independence of the bins and the greater than Poissonian variations in the galaxy surface density due to clustering. Candidate cluster positions are identified as minima in the  $\chi^2$  map, where  $\chi^2$  is significantly, in terms of  $\sigma(\chi^2)$ , lower than the mean for the whole field.

## 4.2 Results

The strongest detection was centred at pixel co-ordinate (488,499) on the 5C6.75 field, where  $\chi^2$  was  $3.06\sigma$  below the mean  $\chi^2$  for the field. This confirms that the cluster is a  $3\sigma$  detection even after taking into account the increased background density variation from galaxy clustering. There are no other  $3\sigma$  detections within 1.5 arcmin of any of the radio galaxies. The best-fit cluster position, shown on Figure 4, is offset by 23 arcsec ( $\simeq 0.11h^{-1}$  Mpc) from the radio galaxy (478,442). However, running our cluster detection routine on 10 simulated  $L_{cl} = 128$  clusters with the profile from Equation 1 predicts RMS errors in the best-fit position of  $\sim 21$  arcsec, so this offset is not significant.

Having determined a centre for the cluster, we can derive a new estimate of its richness and examine its profile. There are 99 galaxies with  $16 \leq K' \leq 19.5$  within 1.5 arcmin of the fitted cluster centre, an excess of  $34.4 \pm 9.9$  above the background, or an excess  $46.6 \pm 13.4$  above the corrected background, giving  $L_{cl} = 128 \pm 37$  (hence Abell richness  $N_A = 85 \pm 25$ ), almost identical with the estimate when the radio galaxy is assumed to be the centre. The richness can also be estimated from  $\chi^2$  as a function of  $L_{cl}$  for a model cluster placed at the fitted position –  $\chi^2$  is minimum for  $L_{cl} = 136 \pm 26$  (error from the simulation), consistent with the first estimate.

Figure 5 compares the observed cluster profile with the  $L_{cl} = 128$ ,  $R_c = 0.1 h^{-1}$  Mpc model. Allowing both  $L_{cl}$  and  $R_c$  to vary gives a best-fitting core radius as  $R_c = 0.12 \pm 0.03h^{-1}$  Mpc. The agreement of both the observed profile and the best-fit  $R_c$  with the model profile confirms that the

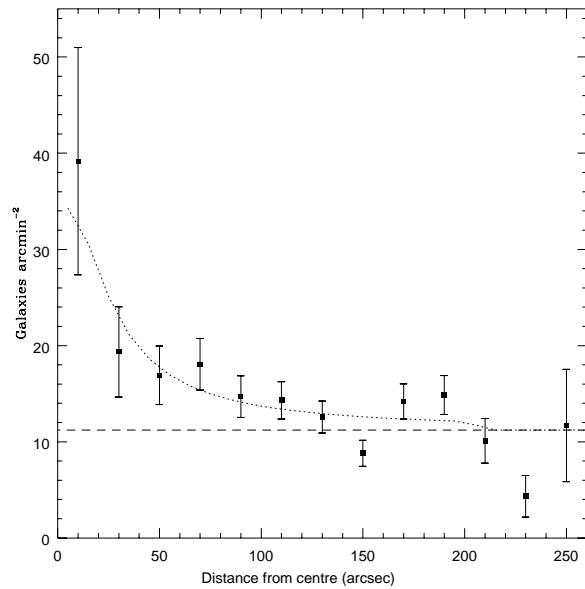


**Figure 5.** Radial density profile of the 5C6.75 cluster, with  $\sqrt{N}$  error bars, compared to (dotted line) a model cluster profile (equation 1) with  $L_{cl} = 128$  and  $R_c = 0.1 h^{-1}$  Mpc.

distribution of galaxies near 5C6.75 is at least consistent with a typical Abell 1/2 cluster at the radio galaxy redshift.

## 5 THE ANGULAR CORRELATION FUNCTION

### 5.1 Calculating $\omega(\theta)$

We investigate the clustering of all the galaxies on these five fields by calculating the angular correlation function,  $\omega(\theta)$ . Our data may not give an entirely unbiased estimate of the field galaxy  $\omega(\theta)$ , due to the presence of known radio galaxies with strong clustering around at least one, but the great majority of detected galaxies will not be associated with the radio sources, so the resulting bias may be very small. For now, we analyse these images as normal field samples, with no distinction between the radio galaxies and other galaxies, but investigate the effect of the 5C6.75 cluster at the end of Section 5.3.

On a field with  $N_g$  detections classed as galaxies (to a chosen magnitude limit), there will be  $\frac{1}{2}N_g(N_g - 1)$  possible galaxy-galaxy pairs. On each field, these pairs are counted in bins of separation of width  $\Delta(\log \theta) = 0.2$ , giving a function  $N_{gg}(\theta_i)$ . For each field  $N_r = 10000$  points were placed at random over the area covered by real data, i.e. avoiding any holes, and the separations of the  $N_g N_r$  galaxy-random pairs, taking the real galaxies as the centres, are similarly counted, giving  $N_{gr}(\theta_i)$ . In addition, the separations of random-galaxy pairs with the randoms as the centres, and the number of random-random pairs, are similarly binned giving  $N_{rg}(\theta_i)$  and  $N_{rr}(\theta_i)$  respectively.

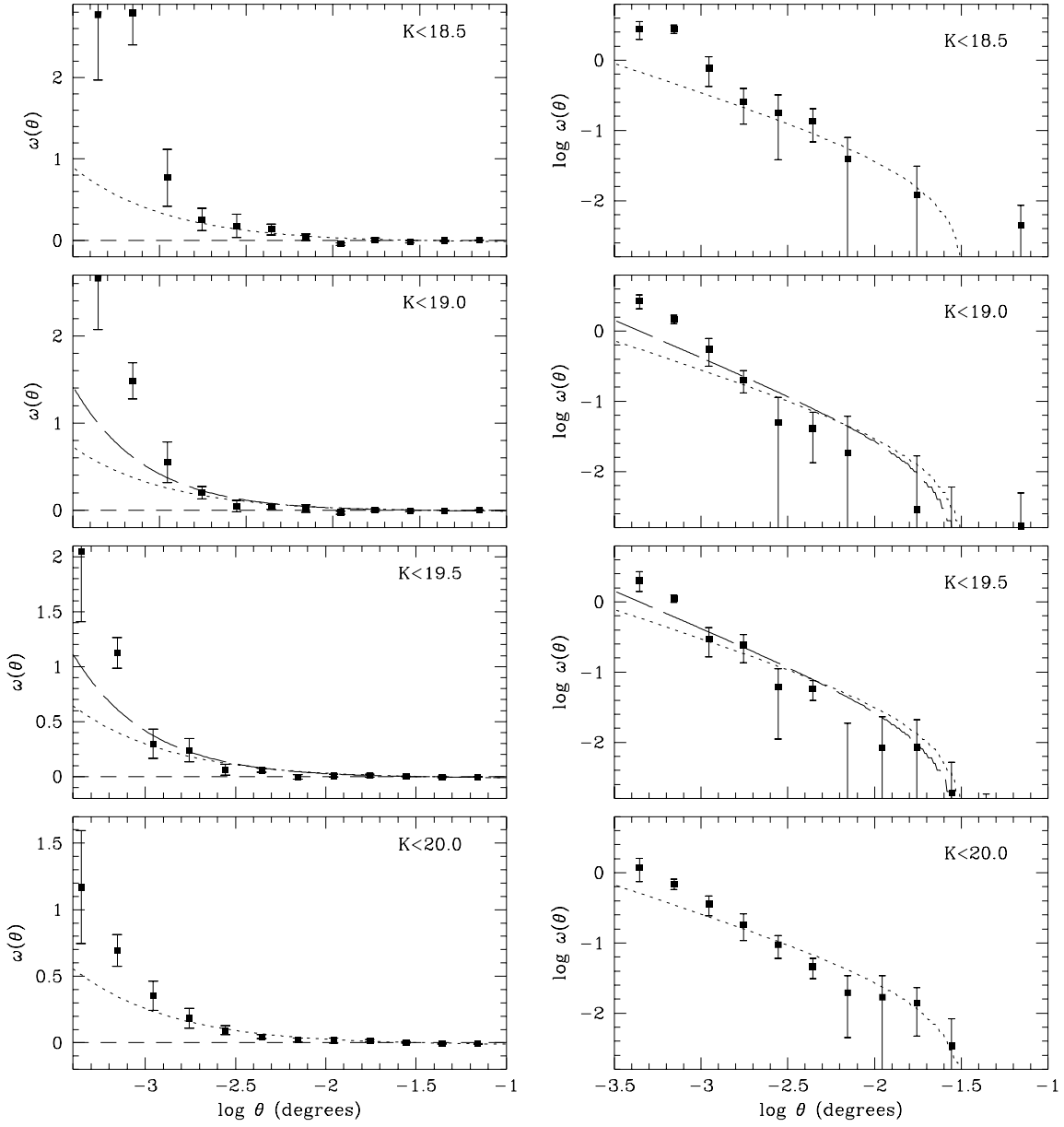


**Figure 6.** Observed  $\omega(\theta)$  for galaxies brighter than  $K' = 18.5, 19.0, 19.5$  and  $20.0$ , as log-linear (left) and log-log (right) plots. The dotted lines show the best-fit  $\theta^{-0.8}$  power-laws with the integral constraint offset. The long-dashed lines show best-fit power-laws with the maximum (from local surveys) slope of  $\theta^{-1.05}$ .

Following Infante and Pritchett (1995) and Roche and Eales (1998), for each of the five fields the galaxy  $\omega(\theta)$  is calculated as

$$\omega(\theta_i) = \frac{N_{gg}(\theta_i)}{N_{gr}(\theta_i)} \frac{2N_r}{(N_g - 1)} - \frac{N_{rg}(\theta_i)}{N_{rr}(\theta_i)} \frac{(N_r - 1)}{2N_g} \quad (5)$$

The five individual field  $\omega(\theta)$  are averaged at each  $\theta_i$  point to give a mean  $\omega(\theta)$ , with error bars from the field-to-field scatter. Figure 6 shows this mean  $\omega(\theta)$  for our five fields, for four magnitude limits.

If the real galaxy  $\omega(\theta)$  is of the form  $A\theta^{-\delta}$ , the observed  $\omega(\theta)$  will follow the form  $\omega(\theta) = A\theta^{-\delta} - C$ , with amplitude  $A$  (defined here at a one-degree separation), and a negative offset  $C$  known as the integral constraint, resulting from the restricted area of the observation.  $C$  can be estimated by doubly integrating an assumed true  $\omega(\theta)$  over an area corresponding to each field, i.e.

$$C = \iint \omega(\theta) d\Omega_1 d\Omega_2 \quad (6)$$

Using the random-random correlation, this calculation can be done numerically –

$$C = \frac{\sum N_{rr}(\theta) \theta^{-\delta}}{\sum N_{rr}(\theta)} \quad (7)$$

As in Paper I we assume a slope  $\delta = 0.8$ , in agreement with most observations including those in the  $K$ -band at brighter limits (Baugh et al. 1996). For these fields,  $\delta = 0.8$  gives  $C = 14.84$ . The  $\omega(\theta)$  amplitude  $A$  is estimated by fitting  $A(\theta^{-0.8} - 14.84)$  to the mean  $\omega(\theta)$  at separations  $2 < \theta < 200$  arcsec. As previously, the error on  $A$  is estimated by fitting the same function to the  $\omega(\theta)$  of the five individual fields and determining the scatter between the individual field amplitudes.

## 5.2 $\omega(\theta)$ results

Figure 6 shows the observed  $\omega(\theta)$  with best-fitting functions of the form  $\omega(\theta) = A\theta^{-0.8} - 14.84$ , and Table 3 gives the amplitudes. There is a significant ( $\sim 4\sigma$ ) detection of galaxy clustering at  $K' = 18.5$ – $20.0$  limits, although the result for  $K' = 20$  may be less reliable due to incompleteness at  $K' > 19.5$  (Section 2.3).

It is apparent that the first two plotted points, corresponding to  $1.26 \leq \theta \leq 3.17$  arcsec, lie above the fitted power-laws, indicating an excess of close pairs. This excess in the small-scale  $\omega(\theta)$  appears very similar to that seen on red-band surveys of comparable depth (Infante et al. 1996; Roche and Eales 1998). There was also some evidence of an excess of 2–3 arcsec pairs on the  $K$ -band Redeye data of Paper I. This was attributed to the effects of galaxy mergers, but it was also suggested in Paper I that  $\omega(\theta)$  from  $K$ -band surveys might be steeper than  $\theta^{-0.8}$ , due to a particularly steep two-point correlation function,  $\xi(r)$ , for giant ellipticals. Redshift surveys will give better constraints on the slope of  $\xi(r)$  than our small dataset. Loveday et al. (1995) found a  $\xi(r)$  slope  $\gamma = 1.87 \pm 0.07$  for E/S0 galaxies and Guzzo et al. (1997) a more extreme  $\gamma = 2.05 \pm 0.09$  for higher luminosity E/S0s. The latter estimate corresponds to  $\theta^{-1.05}$ , which we assume as an extreme upper limit to the possible range of slopes, and fit ‘ $A(\theta^{-1.05} - C)$ ’ (where

**Table 3.** Observed  $\omega(\theta)$  amplitudes ( $A$ ), in units of  $10^{-4}$  at  $1^\circ$ , the number of galaxies ( $N_{gal}$ ), the estimated fraction of contaminating stars  $f_s$  and the  $\omega(\theta)$  amplitudes  $A_{corr}$ , with a correction for star contamination, at a series of  $K'$  magnitude limits

$K'$ limit	$A$	$N_{gal}$	$f_s$	$A_{corr}$
18.5	$14.54 \pm 2.01$	807	0.186	$21.94 \pm 3.03$
19.0	$11.80 \pm 3.01$	1117	0.180	$17.55 \pm 4.48$
19.5	$12.61 \pm 2.30$	1626	0.157	$17.76 \pm 3.24$
20.0	$10.91 \pm 2.20$	2110	0.140	$14.74 \pm 2.97$

$C = 38.19$  for  $\delta = 1.05$  from equation 7), to the observed  $\omega(\theta)$ .

Figure 5 shows this steeper power-law for two of the magnitude limits with the best-fitting amplitude ( $A = 3.03 \pm 0.46 \times 10^{-4}$  at  $K = 19.5$ ,  $A = 3.02 \pm 1.57 \times 10^{-4}$  at  $K = 19.5$ ). Assuming this maximum slope does not get even half-way to fitting the excess in the small-scale  $\omega(\theta)$ , suggesting that the dominant contribution to the close-pair excess must be from mergers and interaction rather than steep E/S0 galaxy clustering. The excess of close pairs is discussed further in Sections 6 and 7.4.

A fraction of (randomly distributed) stars  $f_s$  within the galaxy sample will reduce the observed  $\omega(\theta)$  at all angles by a factor of  $(1 - f_s)^{-2}$ . The number of contaminating stars is estimated as described in Section 2.3, with the incompleteness in star detection at  $19.5 < K' < 20$  assumed to be the same as that (32 per cent) estimated for galaxies. Table 2 gives estimates of the fraction of faint ( $K > 16.5$ ) stars  $f_s$  in the sample of  $N_{gal}$  objects classed as galaxies at each magnitude limit, and amplitudes  $A_{corr}$  corrected for star contamination by multiplying the fitted  $A$  by  $(1 - f_s)^{-2}$ .

It might be thought that the presence of the cluster around 5C6.75 would lead to an upwardly biased estimate of the field galaxy  $\omega(\theta)$ . However, repeating the analysis with the 1.5 arcmin radius area centred on the cluster excluded does not significantly change our results – in units of  $10^{-4}$ , the uncorrected  $\omega(\theta)$  amplitudes become  $11.05 \pm 2.80$ ,  $10.93 \pm 2.50$ ,  $13.79 \pm 2.99$  and  $11.05 \pm 2.74$  at  $K' = 18.5$ ,  $19.0$ ,  $19.5$  and  $20.0$  respectively. Although the  $\xi(r)$  amplitude in the core of Abell 1/2 clusters is several times higher than for field galaxies (see e.g. Hill and Lilly 1991), the excess galaxies within 1.5 arcmin of 5C6.75 amount to only 13 per cent of all galaxies on the CCD frame, which in turn is only one-fifth of our dataset. Hence the effect of their clustering on  $\omega(\theta)$  is greatly diluted and appears to be smaller than our  $1\sigma$  errors.

Figure 7 shows the corrected and uncorrected  $\omega(\theta)$  amplitudes as a function of  $K'$  limit, from this survey and others in the  $K$  band. The Paper I and Carlsberg et al. (1997) results are plotted without a correction for star-contamination, while those of Baugh et al. (1996) are at sufficiently bright magnitudes that star-galaxy separation should be reliable. At  $K = 19.5$ – $20.0$ , our results appear consistent with Paper I. These observations are also compared with models, described below.

## 5.3 Comparison with models

The modelling of  $\omega(\theta)$  amplitudes is discussed in detail elsewhere (e.g. Roche et al. 1996; Roche and Eales 1998; Paper

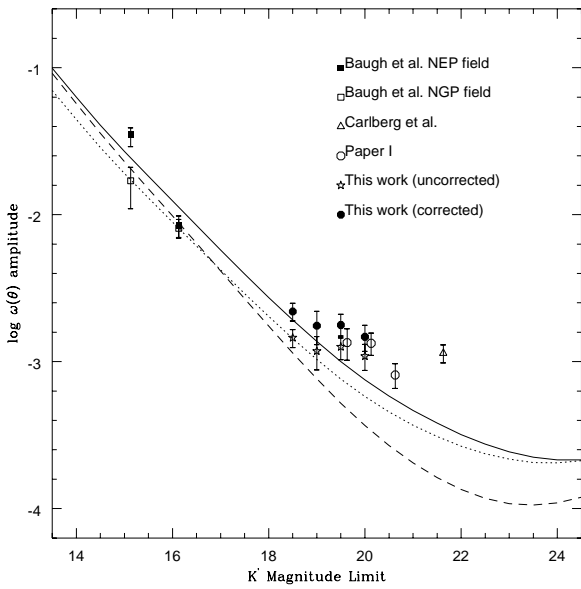


**Figure 7.** The  $\omega(\theta)$  amplitude for galaxies on our five fields, with and without corrections for star-contamination, against  $K'$  magnitude limit, compared with  $\omega(\theta)$  amplitudes from the  $K'$ -band surveys of Baugh et al. (1996), Carlberg et al. (1997) and Paper I. The solid line shows a PLE model (Roche and Eales 1998) with  $r_0 = 8.4 h^{-1}$  Mpc for early-type galaxies and stable clustering ( $\epsilon = 0$ ), the dashed line the same PLE model with  $\epsilon = 1.2$  evolution of the clustering, and the dotted line the  $\epsilon = 0$  PLE model with the strength of clustering from Roche et al. (1996),  $r_0 = 5.9 h^{-1}$  Mpc for E/S0 galaxies.

I) and will be described only briefly here. Essentially, we assume a 3D two-point correlation function for the galaxies of the form

$$\xi(r, z) = (r/r_0)^{-\gamma}(1+z)^{-(3+\epsilon)} \quad (8)$$

where  $r_0$  normalizes the strength of clustering at  $z = 0$ ,  $\gamma$  is the slope and  $\epsilon$  parameterizes the clustering evolution relative to the  $\epsilon = 0$  stable clustering model. This is integrated over a galaxy redshift distribution,  $N(z)$ , using Limber's formula (e.g. Phillipps et al. 1978). Here  $N(z)$  is given by the PLE model of Section 2.3.

Roche et al. (1996) assumed  $\gamma = 1.8$  for all galaxy types, with  $r_0 = 5.9 h^{-1}$  Mpc for E/S0 galaxies and  $r_0 = 4.4 h^{-1}$  Mpc for later types, with an additional luminosity weighting so that dwarf galaxies (those with  $z = 0$  blue-band absolute magnitudes  $M_B > -20.5$ ) are half as clustered as galaxies of higher luminosity (see Loveday et al. 1995). With stable clustering and  $L^*$  evolution, this model predicted a  $\omega(\theta)$  scaling consistent with observations in the blue-band, but in Paper I was later found to underpredict the  $\omega(\theta)$  amplitudes from  $K$ -band surveys at  $K \simeq 19.5-21.5$ . The results from the deep  $K$ -band surveys, in which early-type galaxies will be much more prominent, were better fitted with stronger clustering for early-type galaxies, similar to that observed locally by Guzzo et al. (1997).

The  $\omega(\theta)$  scaling from a large  $R$ -band survey (Roche and Eales 1998), after correction for star-contamination, appeared well-fitted by a PLE model with  $\epsilon = 0$ ,  $\gamma = 1.8$ ,

$r_0 = 8.4 h^{-1}$  Mpc for E/S0 galaxies and  $r_0 = 4.2 h^{-1}$  Mpc for spirals and irregulars, again with  $M_B > -20.5$  galaxies half as clustered as more luminous galaxies. Clustering evolution of  $\epsilon \sim 1.2$ , with the same PLE model, underpredicted the  $\omega(\theta)$  amplitudes and could be rejected by  $\sim 3\sigma$ . On Figure 7, the same PLE model with  $\epsilon = 0$  but with the  $r_0$  from Roche et al. (1996) is seen to underpredict the  $\omega(\theta)$  amplitudes from this survey as well as Paper I, although the rejection is only strong when star-contamination has been taken into account. With the stronger clustering of early-type galaxies from Roche and Eales (1998), the new PLE model, with  $\epsilon = 0$ , predicts higher  $\omega(\theta)$  amplitudes much more consistent with the observations, but with clustering evolution of  $\epsilon = 1.2$  it greatly underpredicts the  $\omega(\theta)$  of deep  $K$ -band surveys, and at  $K' = 19.5$  is rejected by  $> 3\sigma$  even before correcting for star-contamination. Beyond the limits of our survey, the  $\omega(\theta)$  amplitude from the small area studied by Carlberg et al. (1997) exceeds even the  $\epsilon \sim 0$  model, which might suggest a negative  $\epsilon$  at the highest redshifts ( $z \geq 1.5$ ), but more data is needed to confirm this.

In summary, the  $\omega(\theta)$  amplitude from this survey agrees well with previous  $K$ -band observations, favouring both strong ( $r_0 \sim 8.4 h^{-1}$  Mpc) clustering for E/S0 galaxies and clustering remaining stable ( $\epsilon \sim 0$ ) over the observed redshift range. We discuss this further in Section 7.3, after investigating the excess in  $\omega(\theta)$  at  $\theta < 3.2$  arcsec.

## 6 CLOSE PAIRS OF GALAXIES

### 6.1 Introduction

Infante et al. (1996) reported that, for a sample of  $R \leq 21.5$  galaxies, the  $\omega(\theta)$  at  $\theta < 6$  arcsec exceeded the inwards extrapolation of the  $\omega(\theta)$  at large separations by about a factor of 1.8. This excess of close pairs was thought to consist of physically interacting or merging galaxies, with the numbers suggesting that the rate of mergers increased as  $\sim (1+z)^m$  with  $m = 2.2 \pm 0.5$ .

In Paper I, there were found to be about twice as many  $2 \leq \theta \leq 3$  arcsec separation pairs as expected by chance, for the section of the data observed with the Redeye camera ( $41.8 \text{ arcmin}^2$ ), and from this it was estimated that  $8.5 \pm 3.8$  per cent of  $K \leq 20$  galaxies on those fields belonged to close ( $\theta < 3$  arcsec) pairs in excess of the expectation from chance and from the fitted  $\omega(\theta)$ . This result was consistent with similar evolution of the merger rate, but the detection of the excess was of low significance, and no close pair excess was seen on the other half of the data observed with the lower-resolution Magic camera. The much larger  $R$ -band survey of Roche and Eales (1998) did find a significant excess in the small-scale ( $2 \leq \theta \leq 5$  arcsec) on one of two fields studied, corresponding to  $12.88 \pm 4.05$  per cent of  $R < 23.0$  galaxies in  $\theta < 5$  arcsec pairs in excess of the expectation from  $\omega(\theta)$  at  $\theta > 5$  arcsec, but found no significant excess of close pairs on the second field. In view of these inconsistent results, it is important to investigate the close pair statistics of other deep surveys.

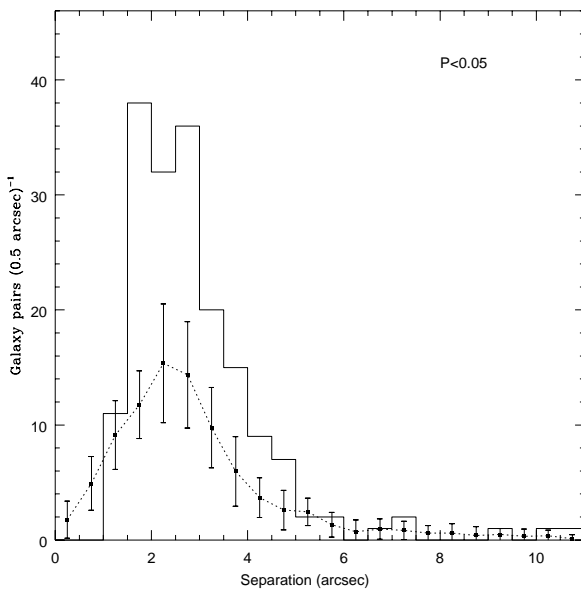


**Figure 8.** Histograms of the observed numbers of galaxy-galaxy pairs (to  $K' = 19.5$ ) with probability  $P < 0.05$ . The dotted line shows the pair count from simulated random distributions of galaxies, with error bars from the simulations.

## 6.2 Method

The  $\omega(\theta)$  from this data showed a significant excess at  $1.26 \leq \theta \leq 3.17$  above the fitted power-law (Figure 5), indicating that a close-pair excess is observed. As in paper I, this is quantified using a method described by Woods, Fahlman and Richer (1995). A probability  $P$  of occurring by chance (in a random distribution of galaxies) is estimated for each galaxy-galaxy pair, as

$$P = \int_{\beta}^{\theta} \exp(-\pi \rho \alpha^2) d\alpha \quad (9)$$

where  $\rho$  is the surface density of galaxies brighter in apparent magnitude than the fainter galaxy of the pair,  $\theta$  is the pair separation and  $\beta$  an angular separation cut-off below which individual objects cannot be resolved.

As in Paper I we take  $\beta = 1$  arcsec and find the area around each galaxy by counting randomly distributed points in annular bins rather than assuming  $\pi r^2$ , thus taking into account field edges and holes. For all 1629 objects classed as galaxies to the estimated completeness limit  $K' = 19.5$ , we count the number of pairs with  $P \leq 0.05$  in  $\delta(\theta) = 1$  arcsec bins of separation. The same analysis is performed on 25 randomized datasets in which the ‘galaxies’ have the same magnitudes but are redistributed randomly over the field areas. The pairs counts from the randomized dataset are averaged, and their scatter used to derive error bars for a single dataset.

## 6.3 Results

Figure 8 shows a histogram for the  $P \leq 0.05$  pair counts compared to the random expectation. The number of pairs exceeds the random expectation by a factor of  $\sim 2.5$  over the  $1.5 < \theta < 5.0$  arcsec range, in which there are 157 pairs

with  $P \leq 0.05$  compared to  $63.48 \pm 10.57$  expected for a random distribution of galaxies. The excess above random, assuming the error to scale as  $\sqrt{N}$ , consists of  $93.52 \pm 16.62$  pairs. One one field, every pair was examined by eye and the great majority appeared to be genuine galaxy pairs, in many cases interacting, only 2 out of 38 appeared spurious (caused by irregular outer regions of bright galaxies). There are 15  $1.5 < \theta < 5.0$  arcsec pairs within 1.5 arcmin of the cluster radiogalaxy 5C6.75, compared to 3.16 expected by chance, or 7.8 if the ratio of observed pairs to the random expectation is the same as for the whole dataset. The cluster may then add a few more excess pairs, simply as its galaxies are closer together, but is only a minor (< 10 per cent) contributor to the overall result.

No  $\theta < 1$  arcsec pairs are counted on any field, as they would be merged into a single detection with the  $\text{FWHM} \simeq 1.13$  arcsec resolution. At  $1.0 < \theta < 1.5$  arcsec, the number of detected pairs is approximately the random expectation, suggesting (by comparison with  $1.5 < \theta < 2.0$  arcsec separations) that about 60 per cent are merged. As in Paper I, the number of close pairs missed due to image merging is estimated by (i) assuming that all pairs above a separation  $\theta_{min}$ , here 1.5 arcsec, are resolved, (ii) extrapolating the excess pairs count inwards from the number at  $\theta > \theta_{min}$ , assuming a  $\theta^{-0.8}$  power-law for the small-scale  $\omega(\theta)$ . This predicts the number of pairs above the random expectation at  $\theta < 1.5$  arcsec to be 0.3068 the number at  $1.5 < \theta < 5.0$  arcsec.

To estimate the number of physically merging or interacting galaxies, we need to subtract from the excess of pairs above the random expectation, the number of pairs expected from the normal galaxy clustering. Clustering with a  $\theta^{-0.8}$  power-law of amplitude  $\alpha$  at 1 arcsec would increase the number of  $\theta < 5$  arcsec pairs above the random expectation by a factor

$$\frac{\int_0^5 2\pi\theta\alpha\theta^{-0.8} d\theta}{\pi(5)^2} = \frac{2\pi\alpha}{25\pi} \frac{\theta^{1.2}}{1.2} = 0.46\alpha \quad (10)$$

At  $K' = 19.5$ , our measured  $\omega(\theta)$  amplitude corresponds to  $\alpha = 0.88 \pm 0.16$  without correction for star-contamination or  $\alpha = 1.24 \pm 0.23$  with correction, and the random expectation for  $\theta < 5$  arcsec pairs is 79.28.

First neglecting star-contamination, the excess of  $\theta < 5$  arcsec pairs above the expectation from chance plus the larger scale  $\omega(\theta)$  amounts to  $1.3086 \times (93.52 \pm 16.62) - 0.46 \times (0.88 \pm 0.16) \times 79.28 = 90.99 \pm 22.52$ .

As each pair consists of two galaxies, the fraction of the 1629 galaxies in merging/interacting pairs is then  $(2 \times 90.99 \pm 22.52)/1629 = 11.2 \pm 2.8$  per cent. Taking into account the estimated star contamination, the excess of  $\theta < 5$  arcsec pairs is reduced to  $1.3086 \times (93.52 \pm 16.62) - 0.46 \times (1.24 \pm 0.23) \times 79.28 = 77.16 \pm 23.31$ , but the number of galaxies is also reduced, to 1373, leading to a similar estimate of the merging/interacting fraction, as  $(2 \times 77.16 \pm 23.31)/1373 = 11.2 \pm 3.4$  per cent. This estimate is discussed further in Section 7.3.

## 7 DISCUSSION

### 7.1 Radio galaxy clustering environment

We investigated the clustering environment of a small sample of 5 radio galaxies at  $0.7 < z < 0.8$ . In Paper I, we were able only to set upper limits of the strength of clustering around radio galaxies at  $z_{mean} \simeq 1.1$ , but with this sample, due to the more moderate redshifts and the use of larger CCD fields, we are more successful. We detect at  $\geq 3\sigma$  significance a cluster, estimated to be of Abell richness class 1 or 2, around the radio galaxy 5C6.75. The cluster, with a total Abell richness  $N_A = 85 \pm 25$ , had a profile consistent with a typical rich cluster ( $R_c \simeq 0.1 h^{-1}$  Mpc,  $\alpha \simeq 0.75$  in equation 1) at the radiogalaxy redshift. The other four radiogalaxies were not in Abell-type clusters – two appeared to be in less rich groups or structures, and two in field environments.

Whereas luminous radio galaxies at low redshifts tend not to be found in clusters, Hill and Lilly (1991) found that a sample of 43 radio galaxies at  $0.35 < z < 0.55$  were distributed in similar numbers over field, Abell 0 and Abell 1 environments. The mean clustering environment, quantified in terms of the normalization of  $\xi(r)$ , was  $B_{gg} = 291 \pm 45$ , approximately that of an Abell 0 cluster. The sample covered a very wide range of radio luminosity, including the luminosity range of our 7C galaxies. There was no strong dependence of cluster environment on radio luminosity – for the most luminous (3C) subsample the mean was  $B_{gg} = 342 \pm 96$ . It was concluded that the mean  $B_{gg}$  of luminous (FRII) radio galaxies – not only 3C sources but those with more moderate radio luminosities similar to our 7C sample – increased by approximately a factor 2.5 from  $z \sim 0$  to  $z \sim 0.5$ . We aim to determine whether there is a further increase at  $z > 0.5$ .

In Paper I a  $1\sigma$  upper limit  $B_{gg} \leq 587$  was estimated for 17 radio galaxies at  $z \sim 1.1$ . Deltorn et al. (1997) found that radio galaxy 3CR184 at  $z = 0.996$  was in a rich, massive cluster of Abell class 1 or 2. Bowes and Smail (1997) detected, by gravitational lensing, a cluster of similar mass around a radio-loud QSO 3C336 at  $z = 0.927$ , but found no significant lensing signal for 7 other very luminous (3C) radio galaxies at  $0.87 < z < 1.05$ , indicating a mean environment no richer than a typical Abell 1 cluster. Similarly, we find one radio galaxy of our sample to be in an Abell class 1 or 2 cluster and can only set upper limits on the clustering around the others.

We estimated the mean Abell richness of the environment of our  $0.7 < z < 0.8$  radio galaxies as  $N_A = 29 \pm 14$ . For a large survey of clusters, Lubin and Postman (1997) find  $N_A \simeq 2.5\text{--}2.7 N_0$ , where  $N_0$  is the core ( $< 0.25 h^{-1}$  Mpc) richness, and Hill and Lilly (1991) fit  $B_{gg} \simeq 30N_0$ . Combining these two relations, our estimate corresponds to a mean  $B_{gg} = 335 \pm 162$ , consistent with the Hill and Lilly (1991) estimate for  $0.35 < z < 0.55$  radio galaxies.

Although a larger sample of radio galaxies will be required to confirm this, our results together with those from Paper I and from Bowes and Smail (1997) all suggest there is little or no further evolution in the distribution of luminous radiogalaxy environments from  $z = 0.5$  to  $z = 1$ . Wan and Daly (1996) explain the evolution in the mean environment of FRII radiogalaxies between  $z = 0$  and  $z = 0.5$  as being due to an increase with time in the typical intra-cluster medium pressure; once the pressure reaches a critical threshold FRII activity is suppressed and only the much less

radioluminous FRI outbursts will occur, so FRIIs tend not to be found in lower redshift clusters. If FRI radiogalaxies are not affected in this way their distribution will approximately reflect the range of environments of massive black holes capable of radio outbursts. Hence, if at some high redshift, all clusters have a pressure below the critical threshold for FRII suppression, the distribution of FRII environments should then be similar to that of FRI radiogalaxies at low redshifts. These lie in a wide range of field and cluster environments with the mean richness being about that of an Abell class 0 cluster (Prestage and Peacock 1988; Hill and Lilly 1991; Zirbel 1997). On the basis of the Wan and Daly (1996) model, the rising trend with redshift in the mean clustering environment of powerful radio galaxies would then approach – but not exceed – an Abell 0 cluster at high redshifts, and, as the Abell 0 value appears to have been reached at  $z \sim 0.5$ , we would expect little further change at higher redshifts. This is consistent with our observations.

The disappearance of cluster-environment suppression of the more powerful radio bursts beyond  $z \sim 0.5\text{--}0.6$  would also help to explain why  $> 0.6$  radio galaxies show a much tighter correlation between radio luminosity and host galaxy mass than those at lower redshifts (Eales et al. 1997; Roche, Eales and Rawlings 1998).

### 7.2 The $\omega(\theta)$ amplitude at $K' \sim 19.5$

At magnitude limits  $K' = 19\text{--}20$ , we detect galaxy clustering at  $\sim 4\sigma$  significance. In Paper I we interpreted the relatively high  $\omega(\theta)$  amplitude at  $K \sim 20$  as evidence that the red early-type galaxies were much more clustered than spirals, even at  $z \sim 1$ , and followed a stable clustering ( $\epsilon \sim 0$ ) model. This paper's results support these conclusions at better statistical significance. The  $K$ -band  $\omega(\theta)$  scaling is reasonably consistent with a PLE model with  $\epsilon = 0$  and  $r_0$  of  $4.2h^{-1}$  Mpc for spirals,  $8.4h^{-1}$  Mpc for E/S0 galaxies. The high  $\omega(\theta)$  amplitude and its slow decline on going faintward strongly favour  $\epsilon \sim 0$  and disfavour clustering evolution of  $\epsilon \sim 1.2$  by  $\sim 3\sigma$ .

CDM models with  $\Omega = 1$  predict  $\epsilon \simeq 1\text{--}1.5$  for the mass distribution over the redshift range of our survey (Col/lin, Carlberg and Couchmann 1997; Moscardini et al. 1998), whereas the inferred  $\epsilon \sim 0$  is more consistent with low  $\Omega$  cosmologies. In the models of Moscardini et al. (1998),  $\Omega = 1$  would only be consistent with  $\epsilon \sim 0$  for galaxies out to  $z \sim 1\text{--}2$  if there is strong evolution of the biasing of galaxies relative to the mass distribution, but this possibility appears to be ruled out by the low  $\omega(\theta)$  amplitude on the Hubble Deep Field.

At shorter wavelengths, the  $\omega(\theta)$  from the larger  $R \leq 23.5$  survey of Roche and Eales (1998) is consistent with the same PLE model with the same  $r_0$  and a best fitting  $\epsilon = -0.12 + +0.46_{-0.38}$ , and the  $\omega(\theta)$  in even larger  $I < 23$  survey of Postman et al. was best-fitted with a rather similar model with the CFRS  $N(z)$ ,  $\epsilon = -0.20 \pm 0.17$  and a mean  $r_0 = 5.6 \pm 0.23h^{-1}$  Mpc. Whereas the  $R$ -band survey will be dominated by late-type galaxies, most of the higher redshift galaxies in a  $2.1\mu\text{m}$  survey will be red E/S0s (Figure 3). Hence the consistent estimates of  $\epsilon$  from surveys of similar depth in  $R$ ,  $I$  and  $K'$  would suggest  $\epsilon \sim 0$  for both E/S0 and spiral populations, with the former  $\sim 0.5$  dex more clustered at all redshifts. This is consistent with the Neuschaefer et

al. (1997)  $\omega(\theta)$  of morphologically divided galaxies, where the bulge galaxies remain  $\sim 0.5$  dex more clustered than disk galaxies over the  $18 < I < 24$  range. With deep multi-passband surveys (e.g.  $B$ ,  $R$  and  $K$ ) it should be possible to confirm this by separating galaxy types to high redshift in much larger surveys and comparing their clustering evolution directly.

### 7.3 The evolution of the galaxy merger rate

We also find a highly significant excess of close (1.5–5.0 arcsec separation) pairs of galaxies over the random expectation on these fields. Although this would be expected for any clustered distribution, the number of close pairs also exceeds, at  $\sim 3.3\sigma$  significance, the expectation from the inward extrapolation of the fitted  $\omega(\theta)$ . Even if the observations are fitted with a steeper power-law of  $\omega(\theta) \propto \theta^{-1.05}$ , corresponding to the steepest slope measured for the  $\xi(r)$  of any type of galaxy (Guzzo et al. 1997), the  $\omega(\theta)$  at  $\theta < 3.2$  arcsec still shows an excess over the power-law (Figure 6).

After making a correction for the number of  $\theta \leq 1.5$  arcsec pairs missed due to image merging, we estimate that  $11.2 \pm 3.4$  per cent of  $K' \leq 19.5$  galaxies belong to  $\theta < 5$  arcsec pairs in excess of the fitted  $\omega(\theta)$ . This is consistent with the pair fraction estimates from both the Redeye data of Paper I at  $K \leq 20$  ( $8.5 \pm 3.8$  per cent) and from the field ‘e’ of Roche and Eales (1998) at  $R \leq 23$  ( $12.88 \pm 4.05$  per cent). The clear detection of an excess of close pairs on our relatively high resolution (FWHM  $\simeq 1.13$  arcsec) data suggests that the non-detection of excess pairs on the Magic fields of Paper I and field ‘f’ of Roche and Eales (1998) was the result of the poorer resolution (FWHM  $\sim 1.8$  arcsec) of these datasets, resulting in many images of close pairs becoming merged.

The fraction of galaxies in close pairs can be interpreted in terms of an evolving merger/interaction rate, parameterized here as  $R_m(z) \propto R_{m0}(1+z)^m$ . Following Roche and Eales (1998), we assume  $f_{pair}(z) \propto R_m(z)$  (on the basis that the merger timescale is much shorter than the Hubble time) and normalize  $f_{pair}$  at  $z = 0$  using the Carlberg et al. (1994) estimate that 4.6 per cent of local galaxies are in pairs of projected separation  $< 19 h^{-1}$  kpc. All such pairs will have an angular separation  $\theta < 5$  arcsec at angular diameter distances  $d_A > 784 h^{-1}$  Mpc, i.e. at  $z > 0.455$  in our chosen cosmology. At lower redshifts, assuming  $\omega(\theta) \propto \theta^{-0.8}$ , the fraction of these close-pair galaxies with  $\theta < 5$  arcsec will be  $(\frac{d_A(z)}{784h^{-1}})^{1.2}$ .

We then model  $f_{pair}$  by summing

$$f_{pair} = f_{pair}(z < 0.455) + f_{pair}(z > 0.455) \quad (11)$$

where

$$f_{pair}(z < 0.455) = 0.046 \frac{\int_0^{0.455} \left(\frac{d_A(z)}{784h^{-1}}\right)^{1.2} N(z)(1+z)^m dz}{\int_0^{0.455} N(z) dz}$$

$$f_{pair}(z > 0.455) = 0.046 \frac{\int_{0.455}^6 N(z)(1+z)^m dz}{\int_{0.455}^6 N(z) dz}$$

over the PLE model  $N(z)$  for  $K' \leq 19.5$  (Figure 3). This predicts  $f_{pair} = 4.3$  per cent for no evolution ( $m = 0$ ), 8.6 per cent for  $m = 1$  and 18.2 per cent for  $m = 2$ , with

the observed  $f_{pair} = 11.2 \pm 3.4$  per cent corresponding to  $m = 1.36^{+0.35}_{-0.50}$ .

This merger rate evolution is consistent with both the  $m = 1.2 \pm 0.4$  estimated by Neuschaefer et al. (1997) from deep ( $I \leq 25$ ) HST data and the  $m = 1.69^{+0.63}_{-0.90}$  of Roche and Eales (1998) at  $R = 21$ –23, and a little lower than the  $m = 2.2 \pm 0.5$  estimated by Infante et al. (1996) from  $R < 21.5$  galaxies. Taken in combination, these surveys may hint at a reduction in  $m$  with increasing depth. Carlberg et al. (1994) predict that  $m$  will be sensitive to  $\Omega$ , but in addition any reduction in the mean mass of galaxies at higher redshift (inevitable if merging is occurring), will cause the merger rate evolution to depart from a simple  $R_m(z) \propto (1+z)^m$  form in that deeper surveys would give lower estimates of  $m$ . For example, a low density Universe with  $\Omega = 0.18$  is predicted to give  $m = 2.2$  at low redshift, falling to  $m = 1.2$  at the redshift where the mean galaxy mass is reduced by 32 per cent. Our results and the others discussed here would be consistent with this model, but inconsistent with the more rapid evolution ( $m = 3.2$ –4.5) expected for  $\Omega = 1$ . To confirm that  $m$  does evolve over the  $\sim 2.2$ –1.2 range will require further high resolution surveys, with multiple passbands to provide photometric redshift estimates, to directly determine  $R_m(z)$ .

## 8 SUMMARY OF CONCLUSIONS

1. We investigate the clustering environment of a sample of 5 radio galaxies at  $0.7 < z < 0.8$ , using large-format  $K'$ -band images from the Omega camera. A cluster is detected at  $3\sigma$  significance around the radio galaxy 5C6.75 at  $z = 0.775$ , and is estimated to be of Abell richness class 1 or 2, with  $N_A = 85 \pm 25$ .

2. Of the other radio galaxies, two appeared to be in small groups and two in the field, with a mean clustering environment for all 5 estimated as  $N_A = 29 \pm 14$  richness. The range of radio galaxy environments and the mean  $N_A$ , approximately that of an Abell 0 cluster, are consistent with those of similarly luminous radio galaxies at  $0.35 < z < 0.55$  (Hill and Lilly 1991), suggesting that there is little further change in the mean cluster environment of powerful radio galaxies beyond  $z \sim 0.5$ .

3. The angular correlation function,  $\omega(\theta)$ , of galaxies on these images showed a positive  $\sim 4\sigma$  signal at limits  $K' = 18.5$ –20.0, with a relatively high amplitude and shallow scaling with magnitude limit which are most consistent with a pure luminosity evolution model in which E/S0 galaxies are much more clustered than spirals ( $r_0 = 8.4$  compared to  $4.2 h^{-1}$  Mpc) and clustering is approximately stable ( $\epsilon \sim 0$ ) to  $1 \leq z \leq 2$ . The same clustering model is consistent with the  $\omega(\theta)$  from other  $K$ -band surveys and the  $R$ -band survey of Roche and Eales (1998).

4. There is a significant excess of close pairs (1.5–5 arcsec separation) of galaxies on these fields compared to the expectation from the inward extrapolation of  $\omega(\theta)$ . To  $K' = 19.5$ , we estimate that  $11.2 \pm 3.4$  per cent of galaxies belong to excess close pairs. This can be explained if the local rate of galaxy mergers and interactions increases with redshift as  $\sim (1+z)^m$  with  $m = 1.36^{+0.35}_{-0.50}$ .

### Acknowledgements

The data reduction and analysis were carried out at the University of Wales Cardiff, using facilities provided by the UK Starlink project, funded by the PPARC. NR acknowledges the support of a PPARC research associateship, CJW a PPARC studentship.

### REFERENCES

Abell G.O., Corwin H.G., Olowin R.P., 1989, *ApJS*, 70, 1.

Baugh C. M., Gardener, J.P., Frenk, C.S., Sharples, R.M., 1996, *MNRAS*, 285, L15.

Bowes R.G., Smail I., 1997, *MNRAS*, 290, 292.

Carlberg R. G., Cowie L. L., Songaila A., Hu E. M., 1997. *ApJ*, 484, 538.

Carlberg R. G., Pritchett C. J., Infante L., 1994. *ApJ*, 435, 540.

Colín P., Carlberg R. G., Couchman H. M. P., 1997. *ApJ*, 490, 1.

Collins C.A., Mann R. G., 1998, *MNRAS*, 297, 198.

Deltorn J.-M., Le Fèvre O., Crampton D., Dickinson M., 1997, *ApJ*, 483, L21.

Djorgovski S. G., et al., 1995, *ApJ*, 438, L13.

Eales S., Rawlings S., Law-Green D., Cotter G., Lacy M., 1997, *MNRAS*, 291, 593.

Eke V.R., Cole S., Frenk C. S., 1996, *MNRAS*, 282, 263.

Gardener J. P., Cowie L. L., Wainscoat, R. J., 1993, *ApJ*, 415, L9.

Girardi M., Biviano A., Giuricin G., Mardirossian F., Mezzetti M., 1995, *ApJ*, 438, 427.

Guzzo L., Strauss M. A., Fisher K., Giovanelli R., Haynes M., 1997, *ApJ*, 489, 37.

Hill G.J., Lilly, S.J., 1991, *ApJ*, 367, 1.

Infante L., de Mello D. F., Menanteau, F., 1996, *ApJ*, 469, L85.

Infante L., Pritchett C. J., 1995, *ApJ*, 439, 565.

Kepner J., Fan X., Bahcall N., Gunn J., Lupton R., 1998, preprint.

Loveday J., Maddox S. J., Efstathiou G., Peterson B. A., 1995, *ApJ*, 442, 457.

Lubin L.M., Postman M., 1996, *AJ*, 111, 1795.

Matarrese S., Coles P., Lucchin F., Moscardini L., 1996, *MNRAS*, 286, 115.

Moscardini L., Coles P., Lucchin F., Matarrese S., 1998, *MNRAS*, in press.

Moustakas L., Davis M., Graham J.R., Silk J., Peterson, B.A., Yoshii Y., 1997, *ApJ*, 475, 445.

Neuschaefer L. W., Ratnatunga K., Griffiths R.E., Casertano S., 1997, *ApJ*, 480, 59.

Oemler A., Dressler A., Butcher H.R., 1997, *ApJ*, 474, 561.

Phillipps S., Fong R., Ellis R. S., Fall S. M., MacGillivray H. T., 1978, *MNRAS*, 182, 673.

Postman M., Lauer T.R., Szapudi I., Oegerle W., 1998, *ApJ*, in press (astro-ph/9804141).

Prestage R., Peacock J. A., 1988, *MNRAS*, 230, 131.

Roche N., Eales S., 1998, *MNRAS*, submitted (astro-ph/9803331).

Roche N., Eales S., Hippelein H., 1998, *MNRAS*, 295, 946.

Roche N., Eales S., Rawlings S., 1998, *MNRAS*, 297, 534.

Roche N., Shanks T., Metcalfe, N., Fong R., 1996, *MNRAS*, 280, 397.

Stanford S.A., Elston R., Eisenhardt P.R., Spinrad H., Stern D., Dey A., 1997, *AJ*, 111, 2232.

Szokoly G.P., Subbarao M.U., Connolly A.J., Mobasher B., 1998, *ApJ* 492, 453.

Waddington I., 1998, preprint (astro-ph/9801149)

Wainscoat R. J., Cowie L., 1992, *AJ*, 103, 323.

Wan L. and Daly R. A., 1996, *ApJ*, 467, 145.

Willott C. J., Rawlings S., Blundell K. M., Lacy M., 1998, *MNRAS*, in press (astro-ph/9807026).

Woods D., Fahlman G., Richer H., 1995, *ApJ*, 454, 32.

Yates M G., Miller L., Peacock J.A., 1989, *MNRAS*, 240, 129.

Yee H.K.C., Ellingson E., 1993, *ApJ*, 411, 43.

Zirbel E. L., 1997, *ApJ* 476, 489.